IEEE Photonics Journal
An IEEE Photonics Society Publication

Open Access

# Physical-Layer Security in Orbital Angular Momentum Multiplexing Free-Space Optical Communications

Volume 8, Number 1, February 2016

**Xiaole Sun**
**Ivan B. Djordjevic**

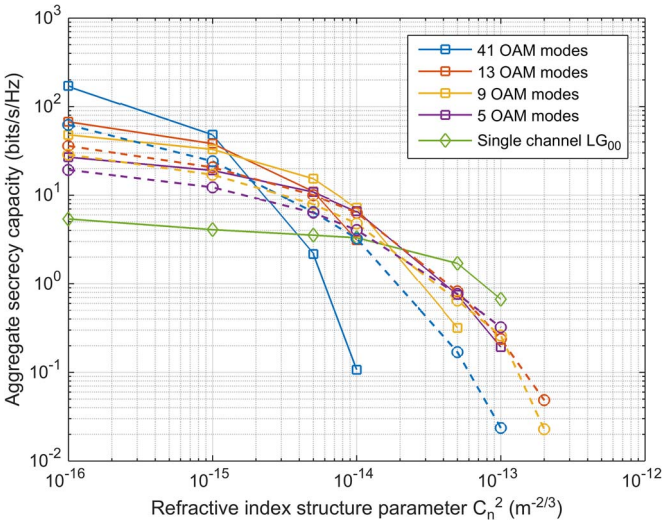


DOI: 10.1109/JPHOT.2016.2519279
1943-0655 © 2016 IEEE

IEEE photonics SOCIETY

IEEE

# Physical-Layer Security in Orbital Angular Momentum Multiplexing Free-Space Optical Communications

**Xiaole Sun**[1] **and Ivan B. Djordjevic**[1,2]

[1]Department of Electrical and Computer Engineering, University of Arizona, Tucson, AZ 85721 USA
[2]College of Optical Sciences, University of Arizona, Tucson, AZ 85721 USA

*DOI: 10.1109/JPHOT.2016.2519279*
*1943-0655 © 2016 IEEE. Translations and content mining are permitted for academic research only. Personal use is also permitted, but republication/redistribution requires IEEE permission. See http://www.ieee.org/publications_standards/publications/rights/index.html for more information.*

Manuscript received December 7, 2015; revised January 12, 2016; accepted January 14, 2016. Date of publication January 19, 2016; date of current version January 29, 2016. This paper was supported by the Office of Naval Research Multidisciplinary Research Initiative (ONR MURI) Program. Corresponding author: X. Sun (e-mail: sunxiaole@email.arizona.edu).

**Abstract:** The physical-layer security of a line-of-sight (LOS) free-space optical (FSO) link using orbital angular momentum (OAM) multiplexing is studied. We discuss the effect of atmospheric turbulence to OAM-multiplexed FSO channels. We numerically simulate the propagation of OAM-multiplexed beam and study the secrecy capacity. We show that, under certain conditions, the OAM multiplexing technique provides higher security over a single-mode transmission channel in terms of the total secrecy capacity and the probability of achieving a secure communication. We also study the power cost effect at the transmitter side for both fixed system power and equal channel power scenarios.

**Index Terms:** Atmospheric turbulence, free-space optical (FSO) communication, physical-layer security, secrecy capacity, orbital angular momentum (OAM) multiplexing.

## 1. Introduction

Free-space optical (FSO) communication, also known as optical wireless communication, is a promising communication technology for high-data-rate information transmission that is available at optical frequencies. Secrecy issues of FSO links have been studied recently for realizing a secure communication between two legitimate peers. Because of the high directionality of laser beam, the FSO communication is more secure than traditional RF wireless communications. However, it could also be susceptible to optical tapping eavesdropping. In [1], physical layer security in FSO links was studied based on an On-Off Keying (OOK) modulation with direct detection scenario. Effects of atmospheric turbulence on the receiving intensity were characterized with well-developed statistical models, e.g., lognormal and Gamma-Gamma distributions. A probabilistic metric for characterizing communication secrecy was presented as probability of strictly positive secrecy capacity. In [2], physical layer security of visible light communications (VLC) is discussed in a broadcasting scenario. Null-steering and artificial noise strategies were utilized to achieve positive secrecy rates when the eavesdropper's channel state information (CSI) is perfectly known or entirely unknown to the transmitter. The secrecy analyzed with such optical tapping channel, also called optical wiretap channel, is typically referred to as information theoretic security (ITS). The ITS scenario has been compared against an extremely secure physical layer security scenario provided by quantum key distribution (QKD) in [3].

From the transmission perspective, orbital angular momentum (OAM) multiplexing technology has been studied and demonstrated to increase the capacity of FSO communications by using OAM beams as carriers [4], [5]. OAM of light is related to the spatial phase profile [6]–[10]. An OAM beam comprising an azimuthal phase term $l\phi$ has an OAM of $l\hbar$ per photon [11]. Since OAM beams with different $l\phi$ values are mutually orthogonal, in principle, there is no interference between multiplexing channels. However, in the presence of atmospheric turbulence, orthogonality between OAM modes is no longer preserved after certain propagation distance. The random refractive index distribution will distort the helical phase fronts of the OAM beam and induce crosstalk between channels. As a result, part of the energy is redistributed into other adjacent OAM modes. This turbulence effect will greatly degrade the performance of the OAM multiplexed FSO communications.

In this paper, we study the FSO channel with OAM multiplexing under different atmospheric turbulence conditions. We numerically simulate the propagation of Laguerre-Gaussian (LG) beam over a turbulent line-of-sight (LOS) link and provide an information theoretic security analysis based on optical tapping scenarios. We show that by using OAM multiplexing, a higher secrecy capacity can be achieved over conventional OOK FSO channels under certain channel conditions, when adaptive optics is not used.

The paper is organized as follows. In Section 2, OAM multiplexing and the propagation of OAM modes over atmospheric turbulence channels are studied. In Section 3, the information-theoretic secrecy capacity of OAM multiplexing is studied assuming the worst-case scenario in which Eve is located on transmitter side, except for Section 3.3. In Section 3.1, the aggregate secrecy capacity of OAM multiplexing is studied for different power allocation strategies. On the other hand, in Section 3.2, the probability of positive secrecy capacity is studied. Further in Section 3.3, the aggregate secrecy capacity is studied assuming that Eve is located on receiver side. Some important concluding remarks are provided in Section 4.

## 2. OAM Beams Multiplexing and FSO Channel Modeling

### 2.1. Generating Information-Carrying Laguerre-Gaussian Beams and Multiplexing

Among the beams that can carry OAM, the Laguerre-Gaussian (LG) beam has a well-defined OAM equal to $l\hbar$ per photon, where $l$ is the azimuthal index. The field distribution of LG mode is given as

$$u(r,\phi,z)=\sqrt{\frac{2p!}{\pi(p+|l|)!}}\frac{1}{w(z)}\left[\frac{r\sqrt{2}}{w(z)}\right]^{|l|}L_p^l\left[\frac{2r^2}{w^2(z)}\right]e^{\left[\frac{-r^2}{w^2(z)}\right]}e^{\left[\frac{-ikr^2z}{2\left(z^2+z_R^2\right)}\right]}e^{\left[i(2p+|l|+1)\tan^{-1}\frac{z}{z_R}\right]}e^{-il\phi} \quad (1)$$

where $w(z)=w_0\sqrt{1+(z/z_R)^2}$ is the beam radius at propagation distance $z$, $w_0$ is the beam waist at $z=0$, $z_R=\pi w_0^2/\lambda$ is the Rayleigh range, $\lambda$ is the wavelength, and $k=2\pi/\lambda$ is the propagation constant. $L_p^l(\cdot)$ denotes the generalized Laguerre polynomial with azimuthal index $l$ and radial index $p$. For $p=0$ and $l\neq 0$, the intensity of a LG mode is a ring. In this paper, we only consider the LG modes with the radial index $p=0$ and denote as $\mathrm{LG}_{l,0}$ mode.

The LG beams are of special interest because they can easily be generated. To generate OAM-multiplexed beam, first, a number of Gaussian beams carrying data information are generated independently from different transmitters, and these beams are then shone onto a series of computer generated holograms (CGHs) or spatial light modulators (SLMs) which are well programmed with interference pattern between reference beam and specific LG beam. The output (or reflected) information-carrying LG beams are then made collinear or optically multiplexed through non-polarizing beamsplitters. The resulting OAM-multiplexed beam is expanded by a telescope and such obtained OAM multiplexed beam is propagated through the FSO channel. At the receiver side, a receiver telescope with aperture diameter $D_{RX}=2w_z\sqrt{|l_{\max}|}$ is used to collect 99.9% of the transmitted power in the absence of turbulence [12], where $w_z$ is the zero-order beam radius at distance $z$, which is followed by a set of mode filters for demultiplexing. In

the absence of atmospheric turbulence, the received field $u_n(r,\phi,z)$ of $\mathrm{LG}_{l=n,0}$ mode and the analyzing field $u_m(r,\phi,z)$ for $\mathrm{LG}_{l=m,0}$ mode satisfy the orthogonality principle:

$$\begin{aligned}\left\langle u_m(r,\phi,z), u_n(r,\phi,z)\right\rangle &= \int r dr d\phi u_n(r,\phi,z) u_m^*(r,\phi,z) \\ &= \begin{cases} 0 & \forall n \neq m \\ \int r dr d\phi |u_n(r,\phi,z)|^2, & n = m \end{cases}\end{aligned} \tag{2}$$

### 2.2. Turbulent FSO Channel Model and Crosstalk Matrix

To study the atmospheric turbulence effects, we simulate the LG-multiplexed beam propagation over a horizontal LOS FSO link with a propagation distance $z = 1$ km. The beam radius of a $\mathrm{LG}_{l,0}$ beam at propagation distance $z$ is given as [13]

$$r_l(z) = \sqrt{w_0^2 + \frac{\lambda^2 z^2}{\pi^2 w_0^2}} \cdot \sqrt{|l|+1}. \tag{3}$$

For a given propagation distance and azimuthal index $l$, the radius has a minimum at $w_0 = \sqrt{\lambda z/\pi}$. Here, we consider the wavelength $\lambda = 1550$ nm; therefore, the beam waist $w_0$ would be 0.022 m. The atmospheric turbulence along the propagation path is modeled by 11 transverse random phase screens with 100 m space in between. Namely, intensive simulations indicate that at least 11 random phase screens are required to model very strong turbulence regime. Each phase screen is generated by means of filtering white Gaussian noise in the spectral domain and then transforming to spatial domain using fast Fourier transform (FFT) with subharmonic information to further improve the low spatial frequency characteristics of the turbulence [14]. The phase power spectral density (PSD) used to generate random phase screens is a modified version of the Kolmogorov spectrum, which includes both inner and outer scales and is given as [15]

$$\Phi_n(\kappa) = 0.033 C_n^2 \left[1 + 1.802\left(\frac{\kappa}{\kappa_l}\right) - 0.254\left(\frac{\kappa}{\kappa_l}\right)^{\frac{7}{6}}\right] \frac{e^{-\kappa^2/\kappa_l^2}}{\left(\kappa^2 + \kappa_0^2\right)^{\frac{11}{6}}} \tag{4}$$

where $\kappa$ is the spatial frequency, $\kappa_l = 3.3/l_0$, $\kappa_0 = 1/L_0$, $C_n^2$ is the refractive index structure parameter which indicates the turbulence strength, and $l_0$ and $L_0$ are the inner and outer scale of the turbulence, respectively. We set $l_0 = 5$ mm and $L_0 = 20$ m. Each phase screen covers a transverse area of 1 m $\times$ 1 m with 1024 $\times$ 1024 grids. Typical realizations of phase screens ranging from weak to strong turbulence regimes are illustrated in Fig. 1 (top), and distorted phase distributions of $\mathrm{LG}_{l=-5,0}$ mode are shown in Fig. 1 (bottom).

Both transmitter and receiver aperture diameters are set to be $D_{TX} = D_{RX} = 2w_z\sqrt{|l_{\max}|}$. We simulate the propagation of $\mathrm{LG}_{l,0}$ modes of the azimuthal index $l$ ranging from –20 to 20 with the radial index $p$ being set to 0 by performing split-step propagation method [16], [17]. For a given $C_n^2$, each received distorted field with OAM mode $l = n \in \{-20, 20\}$ is filtered by the product given in (2). Note that the mode filters at receiver side are designed with diffracted LG modes at propagation distance $z$ to maximize the receive power. The channel efficiency $\eta_{nm}$ is defined as the product given by (2) normalized by transmitted power, which is given as $P_{TX} = \langle u_n(r,\phi,0), u_n(r,\phi,0)\rangle = \int r dr d\phi |u_n(r,\phi,0)|^2$ and gives a 41 $\times$ 41 crosstalk matrix $T$ as follows:

$$T = \begin{bmatrix} \eta_{-20,-20} & \cdots & \eta_{-20,0} & \cdots & \eta_{-20,20} \\ \vdots & \ddots & & & \vdots \\ \eta_{0,-20} & & \eta_{0,0} & & \eta_{0,20} \\ \vdots & & & \ddots & \vdots \\ \eta_{20,-20} & \cdots & \eta_{20,0} & \cdots & \eta_{20,20} \end{bmatrix}. \tag{5}$$

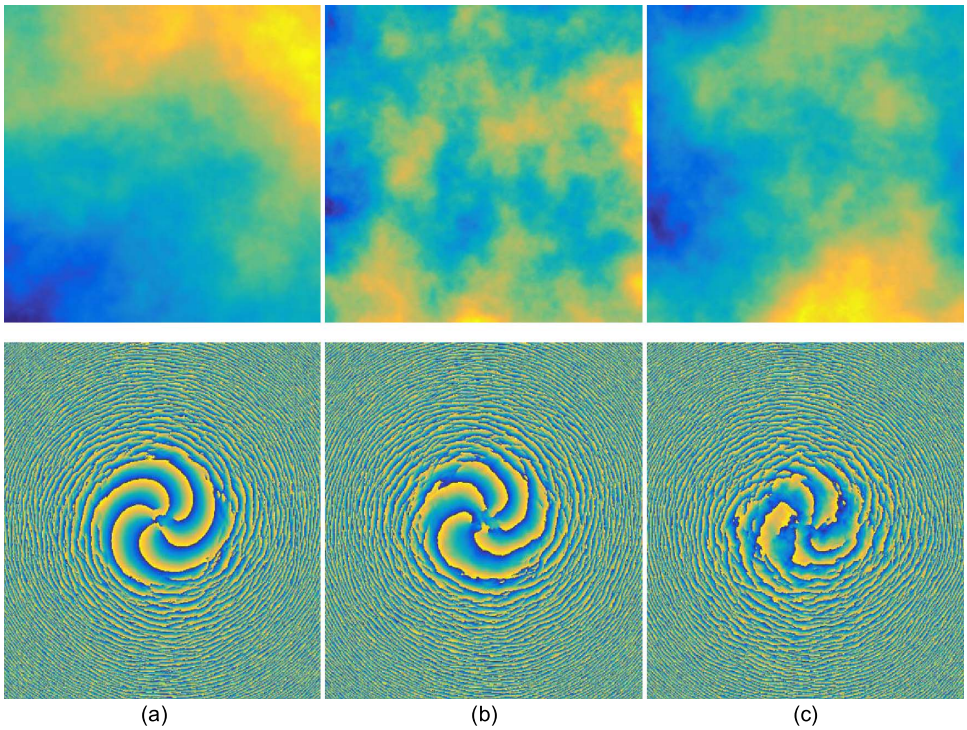


Fig. 1. (Top) Phase screen realizations and (bottom) the distorted phase distribution after propagation of $LG_{l=-5,0}$ mode for different refractive index structure parameters. (a) $C_n^2 = 10^{-15}$ m$^{-2/3}$. (b) $C_n^2 = 10^{-14}$ m$^{-2/3}$. (c) $C_n^2 = 10^{-13}$ m$^{-2/3}$.

In the absence of turbulence, $T$ is an identity matrix. In our simulation, the resulting channel efficiency $\eta_{nm}$ is averaged over 6000 different channel realizations for each turbulence condition.

## 3. Information-Theoretic Secrecy Capacity

The goal is to establish a secure communication in the presence of an external eavesdropper, commonly referred to as Eve. We can reasonably assume that the security is ensured at the transmitter and receiver sides, thus Eve can be allocated anywhere between the transmitter and receiver telescopes. The transmitter and receiver telescope should be well aligned to ensure high efficiency and stability of the system. At the same time, the diameter of telescope aperture is predetermined to collect the vast majority of the transmitter power which, in our case, equals 0.2 m.

From practical implementation point of view, Eve's device will have to intercept the beam. In order to not to be detected by Allice and Bob, the fraction Eve collects $r_e$ should be relatively low so that there would not be a significant continuous reduction of the receiving power at receiver Bob's side. For instance, Eve can use a non-polarizing beamsplitters with a small reflection/transmission (R/T) ratio. The size of commercial non-polarizing cube beamsplitters is typically from 10 mm up to 50 mm. It is difficult for Eve to intercept the whole OAM-multiplexed beam with a regular beamsplitters. In [18] and [19], it has been shown that the recovery of the OAM data is difficult and inefficient when the position of the detector is not directly in the path of the intended receiver. The detection efficiency of OAM beam by using partial receivers is low [20]. These problems impose additional difficulties for Eve compared to traditional modulation formats, such as OOK.

In Fig. 2, we show that the detection efficiency is directly related to the size and position of Eve's intercept device, e.g., the non-polarizing beamsplitter. Apparently, as indicated in Fig. 2(a), the detection efficiency can be increased by using bigger size beamsplitters. The position of the

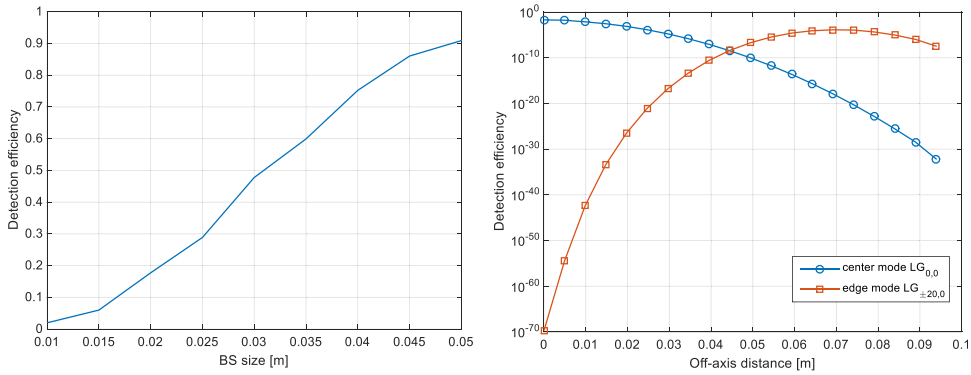


Fig. 2. Detection efficiency of using a cube beamsplitter (BS). (a) Detection efficiency of $LG_{00}$ mode vs. BS size; the BS is placed on-axis. (b) Detection efficiency vs. off-axis distance; the BS size is 10 mm.

beamsplitter matters since the on-axis power vanishes for high azimuthal index LG mode. By putting the beamsplitter off-axis in the annular region where higher order modes have maximum intensity, the detection efficiency reaches its maxima. However, by doing so, the efficiency for center mode, e.g., $LG_{00}$, drops fast as shown in Fig. 2(b). Therefore, in this case, Eve has to use a relatively large size beamsplitter to intercept the entire multiplexed beam for adequate efficiencies in all channels. There are custom commercial beamsplitters available in quite large sizes, which can be up to 300 mm. From the security point of view, we assume that Eve could have the ability to intercept the whole beam without been noticed. The results shown in this paper represent a lower bound in the sense of letting Eve having perfect detection efficiency.

Let us first consider the worst-case scenario when Eve is located close to the transmitter. Intuitively speaking, the closer Eve to the transmitter, the more precise information she can get. In this case, the crosstalk Eve would see in the multiplexed beam is negligible since the signal is intercept before propagating through the whole turbulent free-space channel. For each multiplexed channel, the capacity of the eavesdropper (from Alice to Eve) channel is given as

$$C_{AE} = \log(1 + \gamma_e) \tag{6}$$

where $\gamma_e = P_e/N_0$ is the signal-to-noise ratio (SNR), where $P_e = r_e \cdot P_{TX}$ is the receive power at Eve's end, and $N_0$ is the noise power.

On the other hand, the received beam is distorted by turbulent channel when it arrives at Bob's side. Crosstalk induced by atmospheric turbulence from other channels will contribute to the noise term. As the turbulence strength becomes stronger, the crosstalk between OAM modes is getting more severe. Similarly, the capacity of the transmission (from Alice to Bob) channel can be expressed as

$$C_{AB} = \log(1 + \gamma_b) \tag{7}$$

where $\gamma_b = P_b/N$ is the SNR. Due to the crosstalk, the receive power at the receiver side, which remains in the transmitted LG mode $m$, is given as

$$P_b = (1 - r_e) \cdot P_{TX} \cdot \eta_{mm}^2 \tag{8}$$

where $\eta_{mm}$ is the channel efficiency on the diagonal in (5) for given transmitted LG mode $m$, and the noise term including crosstalk is then given as

$$N = (1 - r_e) \cdot \sum_n \eta_{nm}^2 \cdot P_{TX} + N_0 \quad \forall n \neq m. \tag{9}$$

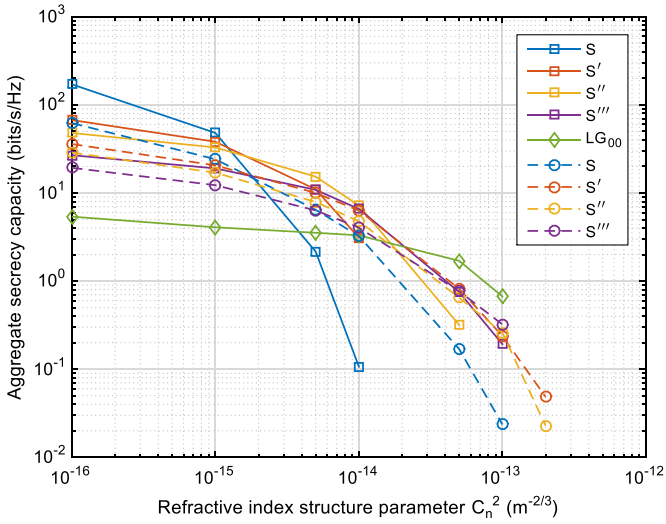


Fig. 3. Aggregate secrecy capacity vs. $C_n^2$. Solid line: equal channel power (ECP); total transmitted power grows with the number of channels. Dash line: fixed system power (FSP); fixed transmitted power is equally divided among OAM channels.

According to the definition given in [1] and [21], the total secrecy capacity is the part which Eve is unable to extract any information and is defined as

$$C_S = C_{AB} - C_{AE} \tag{10}$$

### 3.1. Aggregate Secrecy Capacity: Equal Channel Power vs. Fixed System Power

Aggregate secrecy capacity is the summation of the secrecy capacity for all multiplexed channels. From (9), we can see that, as the turbulence strength grows, the summation of $\eta_{lnm}$ term is getting more relevant and the degradation scenario becomes crosstalk-dominant. In strong turbulence regime, using continuous $LG_{l,0}$ modes could lead to severe degradation in channel capacity [22]. By choosing subsets modes with spacing in between, we can reduce the crosstalk at a cost of using smaller number of multiplexing channels since the total number of LG modes available is predetermined by the size of the receiver telescope aperture. We simulate the propagation of $LG_{l,0}$ modes with continuous azimuthal index $l = n \in S = \{-20, \ldots, -1, 0, 1, \ldots, 20\}$ of total $M = 41$ modes, and pick three subsets to reduce the crosstalk: $S' = \{-18, \ldots, -3, 0, 3, \ldots, 18\}$, $M = 13$, $S'' = \{-20, \ldots, -5, 0, 5, \ldots, 20\}$, $M = 9$, and $S''' = \{-14, -7, 0, 7, 14\}$, $M = 5$ with spacing 2, 4, and 6 between selected modes, respectively.

In Fig. 3, we show the aggregate secrecy capacity by choosing different transmitted mode sets. We assume that the receiver noise powers $N_0$ are the same at both Bob and Eve's end. The power ratio of the transmitter power and the receiver noise power $P_{TX}/N_0$ is set to be 20 dB, and $r_e = 0.01$. As we can see, in the weak turbulence regime, for $C_n^2$ less than $10^{-15}$ $m^{-2/3}$, the total secrecy capacity can be improved by more than one order of magnitude by using OAM multiplexing beam. However, as the refractive index structure parameter $C_n^2$ increases, the secrecy capacity decreases due to orthogonality destruction. Comparing with the secrecy capacity of using single channel, which is shown in Fig. 3 as $LG_{00}$ mode (Gaussian beam), multiplexing beams would not have benefits when turbulence becomes more severe for $C_n^2$ greater than $10^{-14}$ $m^{-2/3}$. Also note that by comparing the solid line for equal channel power (ECP), in which the total power grows linearly with the number of channels $(M \times P_{TX})$, with the dash line for fixed system power (FSP), in which the fixed transmitted power $P_{TX}$ is equally divided among OAM channels, we find that by limiting the power Eve can get, the fixed system power scenario provides higher capacity in the strong turbulence regime.

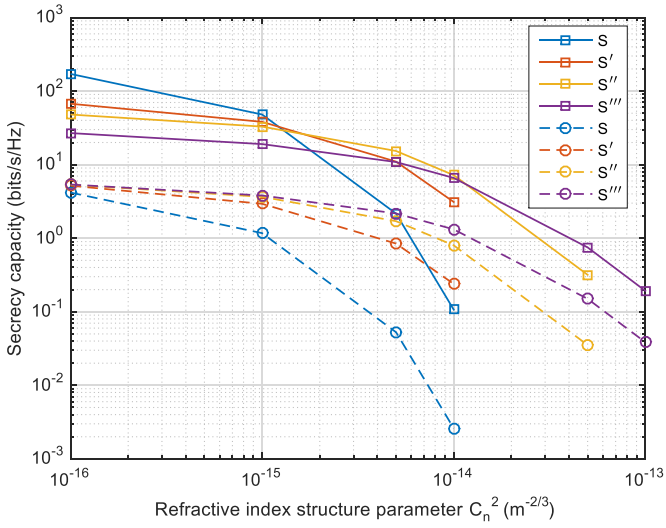


Fig. 4. Secrecy capacity vs. $C_n^2$ for equal channel power (ECP) system; total transmitted power grows with the number of channels. Solid line: aggregate secrecy capacity. Dash line: average secrecy capacity (bits/s/Hz/channel).

Moreover, in order to compare the performance of using different subset modes, average channel capacity is calculated and illustrated together with aggregate channel capacity in Fig. 4. We can easily tell that, with the spacing between selected mode increasing, the average channel secrecy capacity is increasing due to the reduction of crosstalk between multiplexed channels. However, since the total available number of modes is pre-determined by the aperture size of both transmit and receive telescope, using more modes is still beneficial in terms of the aggregate secrecy capacity in weak turbulence regime.

The parameter $r_e$ will also affect the final secrecy capacity. Remember that we consider here the worst case scenario as Eve is at Alice's side so that Eve's signal will not experience the atmospheric turbulence of the transmission channel from Alice to Bob. Additionally, the adaptive optics is not used to deal with atmospheric turbulence effects. In other words, we assume that there is no crosstalk at Eve's side. We also restrict the fraction Eve can intercept up to 10%. Otherwise, Eve would cause a noticeable continuous power reduction at the receiver. In Fig. 5, we illustrate that the aggregate secrecy capacity will decrease as the fraction $r_e$ increases. Clearly, the secrecy capacity drops down as Eve intercepts more power.

Also as we can see in Fig. 5(a), due to the crosstalk induced by turbulence, the aggregate secrecy capacity using multiplexing beams drops below the single channel capacity for Gaussian beam. We can improve the performance by use subsets as shown in Fig. 5(b)–(d). In the weak turbulence regime, e.g., $C_n^2 = 10^{-15}$ $m^{-2/3}$ shown in Fig. 5 in blue, OAM-multiplexing is almost always has the advantage over single Gaussian beam channel. On the other hand, in the strong turbulence regime, i.e., $C_n^2 = 10^{-13}$ $m^{-2/3}$ with yellow lines, achievable secrecy capacity falls below the single Gaussian beam channel for $r_e$ greater than 0.1%. Therefore, in the strong turbulence regime, the adaptive optics approaches should be employed to restore the orthogonality of OAM modes.

### 3.2. Probability of Positive Secrecy Capacity

The effect of atmospheric turbulence is a random process; thus, we could calculate a probabilistic metric for characterizing the secrecy for the communication, which is also known as a *probability of positive secrecy capacity*, and it is defined as [1], [23]

$$P_S^+ = \Pr(C_S > 0) \tag{11}$$

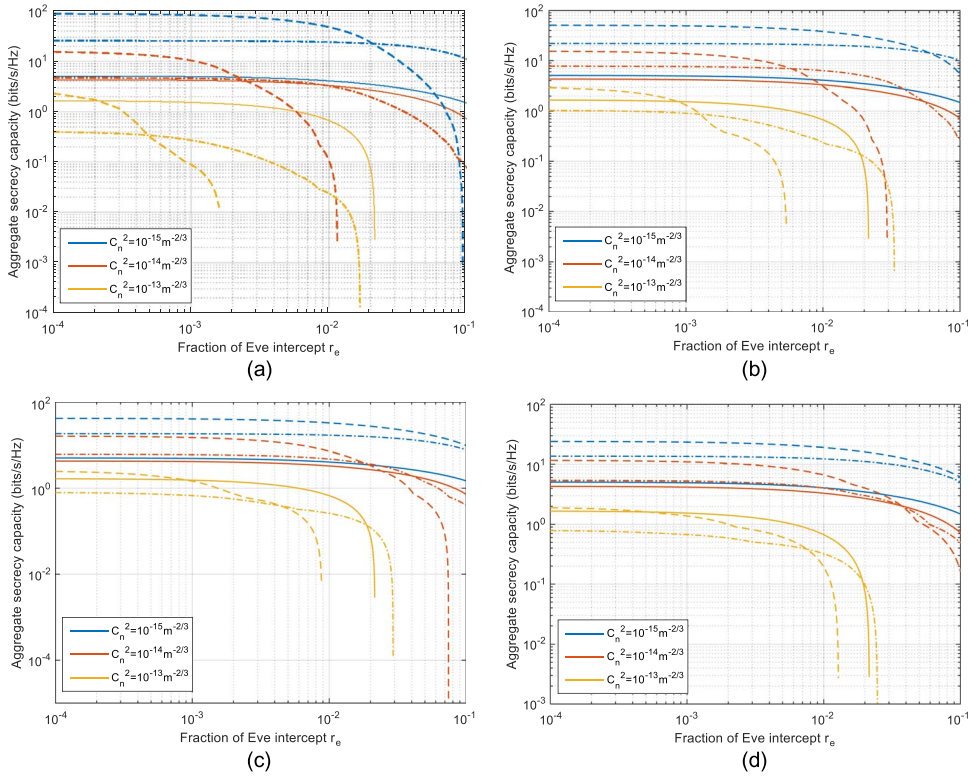


Fig. 5. Aggregate secrecy capacity vs. $r_e$. Solid line: single channel with $LG_{00}$ Gaussian beam. Dash line: equal channel power (ECP). Dash-dot line: fixed system power (FSP). (a) Set S. (b) Subset S′. (c) Subset S″. (d) Subset S‴.

In Fig. 6, subplot (a) shows the probability of positive secrecy capacity in weak turbulence regime, (b) corresponds to medium turbulence, and (c) and (d) correspond to the strong turbulence regime. It is shown that, due to turbulence induced channel crosstalk, the probability of positive secrecy capacity $P_S^+$ decreases faster as $r_e$ increases when turbulence is strong. Note that, since we assume Eve is close to the transmitter, only the transmission channel is affected by the turbulence. In this worst-case scenario, Alice and Bob should limit the total transmitted power to minimize the disadvantage of the channel. In situations when we are limited in transmitted power, the FSP strategy performs better than the ECP with respect to $P_S^+$, as shown in Fig. 6.

### 3.3. Eavesdropper Near the Receiver

So far, we consider the worst-case scenario in which Eve has access to “perfect” OAM channels without suffering from the turbulence. We now consider another scenario in which Eve is located at the receiver side, and her signal will also be distorted by turbulence effects. Here, we still allow Eve to intercept the whole multiplexed beam, which is the same as Bob collection by the receiver (compressing) telescope. The aggregate secrecy capacities are shown in Fig. 7. Compared to the results in Fig. 2, the final secrecy capacity for multiplexing beam is always greater than single-mode channel transmission in the ECP scenario.

## 4. Conclusion

In this paper, we have studied the performance of OAM-multiplexing FSO communication using Laguerre–Gaussian beams as carriers. We have numerically shown that the aggregate secrecy capacity, which defined as the total capacity that Eve cannot obtain any meaningful information,

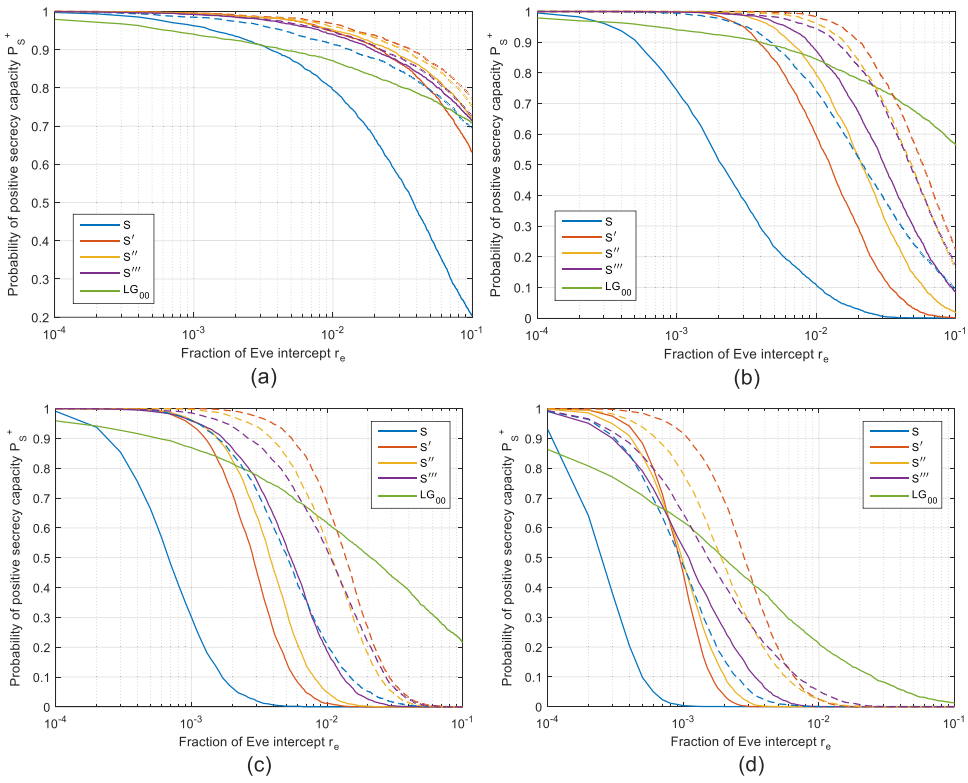


Fig. 6. Probability of positive secrecy capacity $P_S^+$ vs. $r_e$. (a) $C_n^2 = 10^{-15}$ m$^{-2/3}$. (b) $C_n^2 = 10^{-14}$ m$^{-2/3}$. (c) $C_n^2 = 5 \times 10^{-14}$ m$^{-2/3}$. (d) $C_n^2 = 2 \times 10^{-13}$ m$^{-2/3}$. Solid line: equal channel power (ECP). Dash line: fixed system power (FSP).

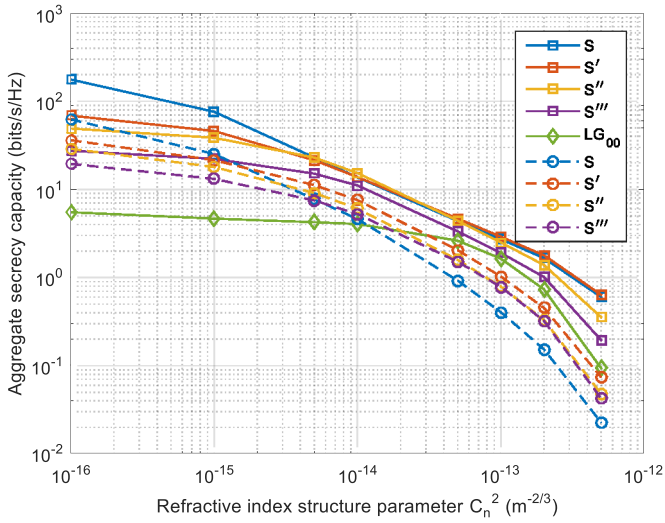


Fig. 7. Aggregate secrecy capacity vs. $C_n^2$. Solid line: equal channel power (ECP). Dash line: fixed system power (FSP).

can be improved by using OAM multiplexing in weak and medium turbulence regimes. Although the secrecy of the system depends on where Eve is located, using LG beam multiplexing with telescope expansion leads to more stringent requirements of Eve's devices. We have also analyzed the physical layer security by using the probability of positive secrecy capacity. We have

shown that, from Eve's perspective, it is better to intercept the beam close to the transmitter. In this case, more information can be obtained by Eve since the orthogonality between channels is still intact. For future research, adaptive optics could be used to improve the signal quality at the receiver and, hence, increase the secrecy capacity in OAM multiplexing channel.

## References


[1] F. J. Lopez-Martinez, G. Gomez, and J. M. Garrido-Balsells, "Physical-layer security in free-space optical communications," *IEEE Photon. J.*, vol. 7, no. 2, Apr. 2015, Art. ID 7901014.

[2] A. Mostafa and L. Lampe, "Physical-layer security for indoor visible light communications," in *Proc. IEEE ICC*, Jun. 2014, pp. 3342–3347.

[3] H. Endo, T. S. Han, T. Aoki, and M. Sasaki, "Numerical study on secrecy capacity and code length dependence of the performances in optical wiretap channels," *IEEE Photon. J.*, vol. 7, no. 5, Oct. 2015, Art. ID 7903418.

[4] J. Wang *et al.*, "Terabit free-space data transmission employing orbital angular momentum multiplexing," *Nature Photon.*, vol. 6, no. 7, pp. 488–496, Jun. 2012.

[5] Y. Yan *et al.*, "High-capacity millimetre-wave communications with orbital angular momentum multiplexing," *Nature Commun.*, vol. 5, p. 4876, Sep. 2014.

[6] J. H. Poynting, "The wave motion of a revolving shaft, and a suggestion as to the angular momentum in a beam of circularly polarized light," *Proc. Roy. Soc., London Ser. A*, vol. 82, no. 557, pp. 560–567, Jul. 1909.

[7] R. A. Beth, "Mechanical detection and measurement of the angular momentum of light," *Phys. Rev.*, vol. 48, p. 471, 1935.

[8] R. A. Beth, "Mechanical detection and measurement of the angular momentum of light," *Phys. Rev.*, vol. 50, no. 2, pp. 115–125, Jul. 1936.

[9] A. H. S. Holbourn, "Angular momentum of circularly polarized light," *Nature*, vol. 137, p. 31, Jan. 1936.

[10] N. Carrara, "Torque and angular momentum of centimeter electromagnetic waves," *Nature*, vol. 164, pp. 882–884, 1949.

[11] L. Allen, M. W. Beijersbergen, R. J. C. Spreeuw, and J. P. Woerdman, "Orbital angular momentum of light and the transformation of Laguerre–Gaussian laser modes," *Phys. Rev. A*, vol. 45, no. 11, pp. 8185–8189, Jun. 1992.

[12] J. A. Anguita, M. A. Neifeld, and B. V. Vasic, "Turbulence-induced channel crosstalk in an orbital angular momentum-multiplexed free-space optical link," *Appl. Opt.*, vol. 47, no. 13, pp. 2414–2429, May 2008.

[13] R. L. Phillips and L. C. Andrews, "Spot size and divergence for Laguerre Gaussian beams of any order," *Appl. Opt.*, vol. 22, no. 5, pp. 643–644, Mar. 1983.

[14] E. M. Johansson and D. T. Gavel, "Simulation of stellar speckle imaging," in *Proc. SPIE, Amplitude Intensity Spatial Interferometry II*, Jun. 1994, pp. 372–383.

[15] L. C. Andrews and R. L. Phillips, *Laser Beam Propagation Through Random Media*, 2nd ed. Bellingham, WA, USA: SPIE, 2005.

[16] D. G. Voelz and J. B. Breckinridge, *Computational Fourier Optics: A Matlab Tutorial*. Bellingham, WA, USA: SPIE, 2011.

[17] J. D. Schmidt, *Numerical Simulation of Optical Wave Propagation With Examples in Matlab*. Bellingham, WA, USA: SPIE, 2010.

[18] G. Gibson *et al.*, "Free-space information transfer using light beams carrying orbital angular momentum," *Opt. Exp.*, vol. 12, no. 22, pp. 5448–5456, Nov. 2004.

[19] G. Xie *et al.*, "Analysis of aperture size for partially receiving and de-multiplexing 100-Gbit/s optical orbital angular momentum channels over free-space link," in *Proc. IEEE GC Wkshps*, Dec. 2013, pp. 1116–1120.

[20] M. Andersson, E. Berglind, and G. Björk, "Orbital angular momentum modes do not increase the channel capacity in communication links," *New J. Phys.*, vol. 17, no. 4, Apr. 2015, Art. ID 043040.

[21] S. Leung-Yan-Cheong and M. Hellman, "The Gaussian wire-tap channel," *IEEE Trans. Inf. Theory*, vol. IT-24, no. 4, pp. 451–456, Jul. 1978.

[22] M. Malik *et al.*, "Influence of atmospheric turbulence on optical communications using orbital angular momentum for encoding," *Opt. Exp.*, vol. 20, no. 12, pp. 13 195–13 200, 2012.

[23] J. Barros and M. D. Rodrigues, "Secrecy capacity of wireless channels," in *Proc. IEEE Int. Symp. Inf. Theory*, Jul. 2006, pp. 356–360.